Unfolded Resonant Converter with Current Doubler Structure Module for Welding Applications

Christian Brañas, Rosario Casanueva, Francisco J. Azcondo
Electronics Technology, Systems and Automation Engineering Department
University of Cantabria
Ave. de los Castros s/n 39005, Santander, Spain
branasc@unican.es

***Abstract*— A new multiphase resonant converter arrangement with series dual phase in the primary side and parallel dual current doubler in the secondary side, operating as a phase shift controlled current source is presented. Sharing the voltage and current stress among the active and passive components with a high DC input voltage and arc current motivates this structure, which also uses WBG devices to increase the efficiency at high switching frequency. The resulting module is intended to operate in continuous and pulsating mode and can be parallelized to extend the output arc current rate.**

Keywords—Arc welding, current multiplier, resonant converter, zero-voltage switching (ZVS).

I. INTRODUCTION

Resonant converters achieve soft, i.e. lossless, switching transitions, pushing the switching frequency and efficiency to higher values and reducing EMI. In bridge configurations, the switching time delay and transient limit the switching frequency because a dead time is required to prevent a shot through situation. The dead time imposes the minimum resonant current phase lag with respect the voltage to ensure the soft turn-on of the power MOSFETs. Also, resonant converters produce higher RMS current values than the square waveforms counterparts, which increases the conduction loss. New wide bandgap devices reduce the switching transient time and the on resistance, meaning a step ahead for the resonant converters process higher power level at higher frequency. Besides these attractive characteristics, the design of the resonant tank can also enhance impedance properties, such as low or high output impedance or power source or sink behavior, especially suitable to supply non-conventional loads [1-2]. Sinusoidal waveforms are also preferred in transformers to limit power loss due to high frequency components. Resonant converters are also appropriate to define modular designs, in which one power conversion section, i.e. a building block, is optimized according to the devices and magnetic components technology and the required dynamic performance. The final converter is defined, according to the volt-amps specification, by connecting different basic blocks. Magnetics are also used to balance the current sharing among the converters.

Arc welding is an application where resonant converters successfully deal with high current and arc stability [3-6]. The high output impedance of the resonant tank imposes the short-term stability of the arc while preserving a fast dynamic response, adequate to implement a fast output current modulation to create pulsating modes. Recently, it has been investigated the effect of pulsating arcs, showing that they reduce the thermally affected zone around the welding threat, increase penetration depth in welding pool and reduce the energy consumption as the pulsating frequency and the di/dt increase [7].

The paper presents a novel approach in the design of resonant converters for arc welding applications. The proposed circuit presents inner modularity in both, the primary inverter section and the secondary rectifier, resulting in a module oriented to be parallelized to reach higher output arc current, as required. Leveraging the wide-band-gap WBG and the modular approach to increase the DC bus voltage, the converter consists of a class D LC_pC_s resonant converter unfolded in two stages with a common midpoint voltage, whose outputs are series coupled in the transformer primary. A series capacitor, C_s decouples any DC component and compensate for the transformer leakage inductance. Operating at constant switching frequency, the total primary transformer current is modulated with the phase displacement between the input voltages to the resonant tanks, achieving zero voltage switching (ZVS) under all load conditions. The secondary rectifier section is designed with a current doubler structure [8-9], also unfolded in two stages connected in parallel at the output to reduce conduction losses. Therefore the transformer connection to the switching structures is series inputs parallel outputs. The welding module is designed to obtain up to 200 A output current with similar efficiency than previously designed 25 A modules [10], operating at the same or higher switching frequency.

II. UNFOLDED RESONANT CONVERTER

In industrial applications at power levels above 1 kW, Boost based three-phase PFC circuits brings some advantages in contrast to its single-phase counterparts [11] however, the DC output voltage is about 1 kV. The high DC link voltage imposes tight design constrains regarding the maximum voltage stress of the switches and it is required a higher

insulation among circuit parts. Moreover, the size of the magnetic components increases also due to the insulation requirements. In order to deal with the high DC link voltage obtained from three-phase PFC circuits, this paper proposes the unfolded resonant converter, whose schematic is shown in Fig. 1. The advantage of the proposed converter is that the voltage applied across the transistors is half of the total DC link voltage. This feature allows to use devices with lower $r_{ds(on)}$, which is critical in high current applications as required for welding machines. Also, splitting the DC input voltage reduce the isolation requirements in the reactive components, increasing the power conversion density.

The secondary side AC-DC conversion stage consists of a current multiplier stage, derived from the current-doubler rectifier [9]. The welding process is modeled according the standard UNE-EN 60974-1 [12], which defines the conventional load voltage for a specific welding process. For example, for an arc welding with coated electrode process (MMA/SMAW) and current of the welding process, I_w, lower than 600 A, the welding voltage, V_w, is defined in steady state as a linear function of I_w so that, $V_w = V_{arc} + R_{arc}I_w$. On the other hand, $V_w = 44$ V if $I_w > 600$ A.

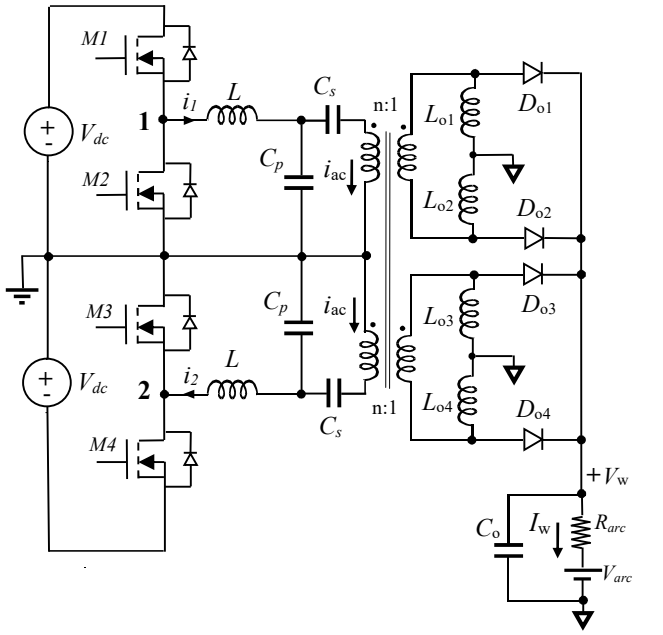

Fig.1. Welding module based on an unfolded LC_pC_s resonant converter with current multiplier as the output stage.

The proposed converter requires a transformer. The transformer is mandatory for safety reasons, as it provides galvanic insolation between the high voltage DC bus and the workpiece. In addition to this, the transformer turns ratio is used as design parameter in order to limit the maximum current in the inverter stage. The structure of the transformer is symmetric, with two primaries and two secondaries, all of them winded in the same magnetic core. The structure of the transformer provides the converter with one interesting feature, as it enables the control of the welding current, I_w, at constant switching frequency by shifting the phase of one inverter output voltage, e.g. v_2, with respect to the other, v_1, as depicted in Fig. 2. The study of the proposed converter is carried out considering the phase angle, Ψ, as the control parameter.

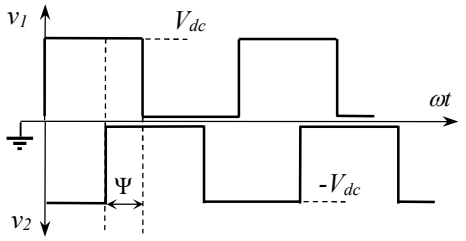

Fig.2. Phase control: output voltages of each inverter section.

A. Output Current Multiplier

The current of the welding process, I_w, circulates trough the output rectifier stage, being a major design issue. In this paper, a current multiplier is used as rectifier stage. The current path for positive and negative semi cycles of the AC current are shown in Fig. 3.

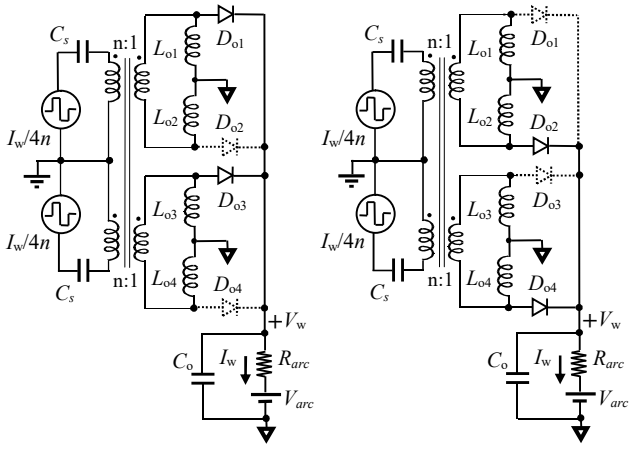

Fig. 3. Output current multiplier. Current path for positive and negative cycles of the AC current.

The current multiplier is obtained from the parallel connection of two current doubler rectifiers [9]. The advantages of this configuration are enhanced with respect to the original current doubler rectifier and are related to lower conduction losses and simplification of the transformer, as each secondary deals with only quarter of I_w.

Since the output filter removes the high frequency ripple, the low ripple approximation [13] is used for modeling the current multiplier stage in steady state. With the first harmonic of a square waveform, the relationship between the AC and DC side currents is given by,

$$I_w = n\pi\hat{I}_{ac}, \tag{1}$$

where $\hat{I}_{ac}$, is the amplitude of the current through the transformer's primary windings and n is the turns ratio (n:1) from each primary to the corresponding secondary winding. The relationship between the AC and DC side voltage is obtained assuming a free loss circuit and each winding handles one half of the output power.

$$V_w = \frac{\hat{V}_{ac}}{n\pi} = R_{arc} I_w + V_{arc} \tag{2}$$

From (1) and (2), the equivalent load of the welding process, seen from each primary winding is,

$$\hat{V}_{ac} = n^2\pi^2 R_{arc}\hat{I}_{ac} + n\pi V_{arc}\,, \tag{3}$$

From (1), (2) and (3) the steady state averaged model of the output current multiplier is shown in Fig. 4

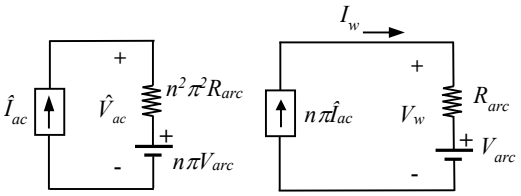

Fig. 4. Steady state averaged model of the current doubler rectifier

From Fig. 4, the rectifier stage is reflected to each transformer's primary winding as the steady-state equivalent resistance given in (4),

$$R_{ac} = \pi^2 n^2 R_w = \pi^2 n^2 \left(R_{arc} + \frac{V_{arc}}{I_w} \right) \tag{4}$$

Assuming steady-state conditions and taking into account that the module is developed for a welding process such as I_w < 600 A, the standard UNE-EN 60974-1 [12] establishes that the constant voltage drop is V_{arc} = 20 V, and the resistor is R_{arc} = 40 mΩ.

III. Steady-State Analysis of the Resonant Inverter

Using the fundamental approximation, the output voltages of each class D section, $v_{1,2}$, are represented in the complex domain by (5) and the equivalent circuit is shown in Fig. 5, where the output current multiplier is reduced to its equivalent impedance, R_{ac}, reflected in the primary sides of the transformer.

$$\mathbf{V_{1,2}} = \frac{2V_{dc}}{\pi} \cdot e^{\pm j\,\Psi/2}\,. \tag{5}$$

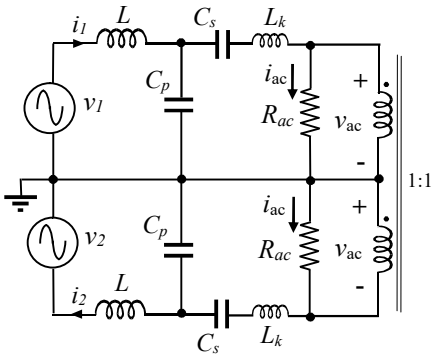

Fig.5. Simplified unfolded LC_pC_s resonant inverter stage for circuit analysis.

In Fig. 5, L_k, represents the leakage inductance of the transformer. The capacitance of the series capacitor, C_s is calculated to achieve, at the switching frequency, the series resonance of L_k-C_s. Then, as the series branch L_k-C_s impedance is null at the switching frequency, the load R_{ac} is connected in parallel with the parallel capacitor C_p as shown in Fig. 6.

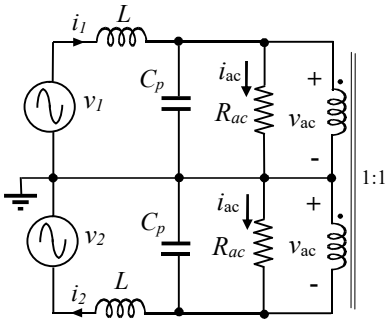

Fig.6. Simplified unfolded LC_p resonant inverter after cancellation of the transformer's leakage inductance.

The main features of the resonant converter in Fig. 6 are defined by the parallel parameters shown in Table I.

TABLE I.
PARAMETERS OF THE UNFOLDED LC_p INVERTER

Parallel Resonant Frequency	Parallel Characteristic Impedance	Parallel Quality Factor
$\omega_p = \frac{1}{\sqrt{LC_p}}$	$Z_p = \omega_p L = \frac{1}{\omega_p C_p}$	$Q_p = \frac{R_{ac}}{Z_p}$

The currents through the resonant inductors i_1 and i_2 are given in a phasor form by (6) where Ω is the normalized switching frequency, $\Omega = \omega/\omega_p$.

(6)

$$\mathrm{I}_{1,2} = \frac{2V_{dc}}{\pi Z_p} \left\{ \frac{\frac{\cos(\Psi/2)}{Q_p} \pm \left(\frac{1}{\Omega} - \Omega\right)\sin(\Psi/2) + j\left[\Omega\cos(\Psi/2) \pm \frac{\sin(\Psi/2)}{Q_p}\right]}{1 - \Omega^2 + j\frac{\Omega}{Q_p}} \right\}$$

The output current amplitude in the AC side of the converter is obtained from (7),

$$\mathrm{I}_{ac} = \frac{2V_{dc}}{\pi Z_p Q_p} \left[\frac{\cos(\Psi/2)}{1 - \Omega^2 + j\frac{\Omega}{Q_p}} \right] \tag{7}$$

The current stability is mandatory in arc welding. On the other hand, some voltage gain capability is necessary in order to produce the dielectric breakdown and stablish the discharge. Both design constraints are fulfilled by designing the resonant converter as a current source. The current source behavior is inherent to the circuit if the switching frequency is set at $\omega = \omega_p$ so that, Ω = 1. After calculating $\hat{I}_{ac}$ in (7) and using (1), the welding current, I_w, is obtained.

$$I_w = \frac{2nV_{dc}}{Z_p}\cos(\Psi/2) \tag{8}$$

From (8), it is verified that the welding current has no dependence on the load. Using (8), the normalized welding

current amplitude as a function of the modulation angle, Ψ, is depicted in Fig 7.

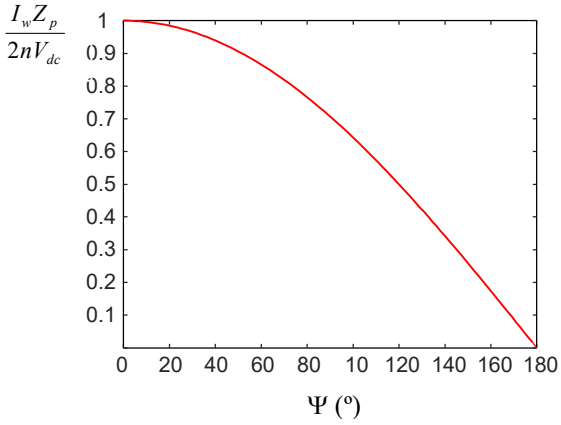

Fig. 7. Amplitude of the normalized welding current, I_w, as a function of the control angle, Ψ.

The modulation angle, Ψ, allow the control of the welding current, I_w, in the full range at constant switching frequency, being maximum for Ψ = 0º and zero for Ψ = 180º. On the other hand, the welding voltage is obtained with $V_w = I_w R_w$ as

$$V_w = \frac{2V_{dc}Q_p}{\pi^2 n}\cos(\Psi/2) \tag{9}$$

The design equations of the converter are derived from (8) and (9). The parallel characteristic impedance, Z_p, is defined to achieve the specified maximum welding current:

$$Z_p = \frac{2nV_{dc}}{I_w}. \tag{10}$$

The transformer turn ratio, n, in (10) is decided as a function of the desired Q_p when I_w is the maximum. From (9),

$$n = \frac{2V_{dc}Q_p}{\pi^2 V_w}. \tag{11}$$

In order to determine the most suitable value of parallel quality factor, Q_p, the switching mode of the transistor is analyzed.

A. Parallel Quality Factor and Transistors Switching Mode

In order to minimize the switching loss the converter is designed to achieve zero-voltage switch (ZVS). The ZVS mode requires a phase lag [13] of the resonant currents, i_1 and i_2, referred to the input voltages v_1 and v_2 for the whole range of the control angle, Ψ. The power factor angles, ϕ_1 and ϕ_2 are obtained from the complex powers, $S_{1,2}$ corresponding to generators v_1 and v_2.

$$S_{1,2} = \frac{2V_{dc}^2}{\pi^2 Z_p}\left\{\frac{\frac{1}{Q_p} \pm \frac{1}{\Omega}\sin(\Psi/2)\cos(\Psi/2) + j\left[\frac{1}{\Omega}\sin^2(\Psi/2) - \Omega\right]}{1-\Omega^2 - j\frac{\Omega}{Q_p}}\right\} \tag{12}$$

From (12) the power factor angles, ϕ_1 and ϕ_2 are obtained as $\phi_{1,2} = \text{angle}(\boldsymbol{S}_{1,2})$ and are strongly dependent on Q_p. The power factor angles ϕ_1 and ϕ_2 are plotted in Fig. 8 as a function of the control angle, Ψ and considering constant the parallel quality factor and the normalized switching frequency so that, $\Omega = Q_p = 1$.

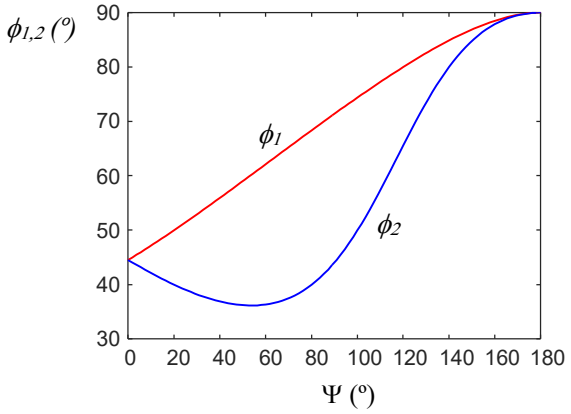

Fig. 8. Power factor angles ϕ_1 and ϕ_2 as a function of the control angle, Ψ. The parallel quality factor and the switching frequency are constant so that, $\Omega = Q_p = 1$.

The value of Q_p defines the ratio active power to reactive power in each inverter section. In this way, a high value of Q_p reduces the reactive energy in the resonant tank and improves the efficiency. For Ψ = 0º, i.e. at maximum output current, both power factor angles are equals as can be observed in Fig. 8. Under such condition (Ψ = 0º) the power factor angles are obtained from (13),

$$\phi_1 = \phi_2 = \arctan\left(\frac{1}{Q_p}\right) = \arctan\left(\frac{2V_{dc}}{n\pi^2 V_w}\right). \tag{13}$$

From (13), it is observed that by increasing the transformer turns ratio, n, the power factor angles diminish then, the reactive energy in the resonant circuit can be reduced. However, a minimum amount of reactive energy must be accepted for assuring the ZVS mode of all transistors. The minimum value of power factor angle ϕ_{zvs} [14] depends on the dead time, t_d, of the driver transistors and the switching frequency.

$$\phi_{zvs} = \frac{\omega_p t_d}{2\pi}\cdot 360^\circ \tag{14}$$

IV. Design of the Resonant Converter

Next, the step-by-step design procedure is summarized.

1) The welding module should provide a maximum current $I_w = 200$ A. According the standard UNE-EN 60974-1, the maximum welding voltage is $V_w = 28$ V for an equivalent load R_w = 140 mΩ. The DC-link voltage obtained from the three-phase PFC input stage is 900 V, so that, each unfold converter is supplied by $V_{dc} = 450$ V.

2) The switching frequency is set at $\omega_p = 2\pi(125\text{kHz})$. Considering a typical value of transistor driver dead time t_d = 700 ns and the switching frequency $\omega_p = 2\pi(125\text{kHz})$, the minimum value of power factor angle is ϕ_{zvs} = 700 ns*125 kHz *360º = 31.4º.

3) The quality factor is chosen to be $Q_p = 1$, which yields at $\Psi = 0^o$ an initial value of the power factor angles $\phi_1 = \phi_2 = 45^o$ achieving, at maximum welding current, a good tradeoff between active and reactive power in each converter. On the other hand, as can be seen in Fig. 8, for $Q_p = 1$, ϕ_1 and ϕ_2 are well above of the minimum value ϕ_{zvs} for the entire range of variation of the control angle Ψ thus, the ZVS is assured for any operation point. According to (11), $Q_p = 0.92$ is achieved for a transformer turn ratio $n = 3$.

4) For $n = 3$, the characteristic impedance is obtained from (10): $Z_p = 13.5\ \Omega$.

5) The reactive components are: $L = Z_p/\omega_p = 17\ \mu H$ and $C_p = 1/\omega_p Z_p = 94.3$ nF.

6) The capacitor C_s is calculated for a transformer's leakage inductance $L_k = 30\ \mu H$ thus, $C_s = 1/L_k\omega_p^2 = 56$ nF.

7) The current multiplier configured with $L_{o1\text{-}4} = 33\ \mu H$, which is enough to remove the high frequency current ripple, and $C_o = 10\ \mu F$.

V. Results

The practical values used are: $V_{dc} = 450V$, obtained from a three-phase PFC stage based on a boost converter, $L = 17\ \mu H$, $C_p = 100$ nF and $C_s = 56$ nF. In order to validate the analysis and design of the proposed converter, the circuit was simulated using the software LTspice IV. The circuit is shown in Fig. 9. The switches model corresponds to C2M0025120D Cree SiC MOSFET transistor and two paralleled CD50065D Cree Schottky SiC Diode. The voltage sources V_7 and V_8 emulate the junction temperature, T_j, as well as the case temperature, T_c, of the transistor. The welding arc is modeled by the voltage source $V_w = 20$ V and $R_{ser} = 40\ m\Omega$.

Some results obtained with simulations with $\Psi = 0^o$ and $\Psi = 90^o$ are shown in Figs. 10 to 15. Figs. 10 and 11 for $\Psi = 0^o$ and Figs. 13 and 15 for $\Psi = 90^o$, show that the resonant currents lag the resonant circuit input voltages, the circuit behavior is inductive and ZVS is achieved. On the other hand, theoretical value and simulation results of the amplitude of the resonant currents as well as the welding current at $\Psi = 0^o$ and $\Psi = 90^o$ are in good agreement.

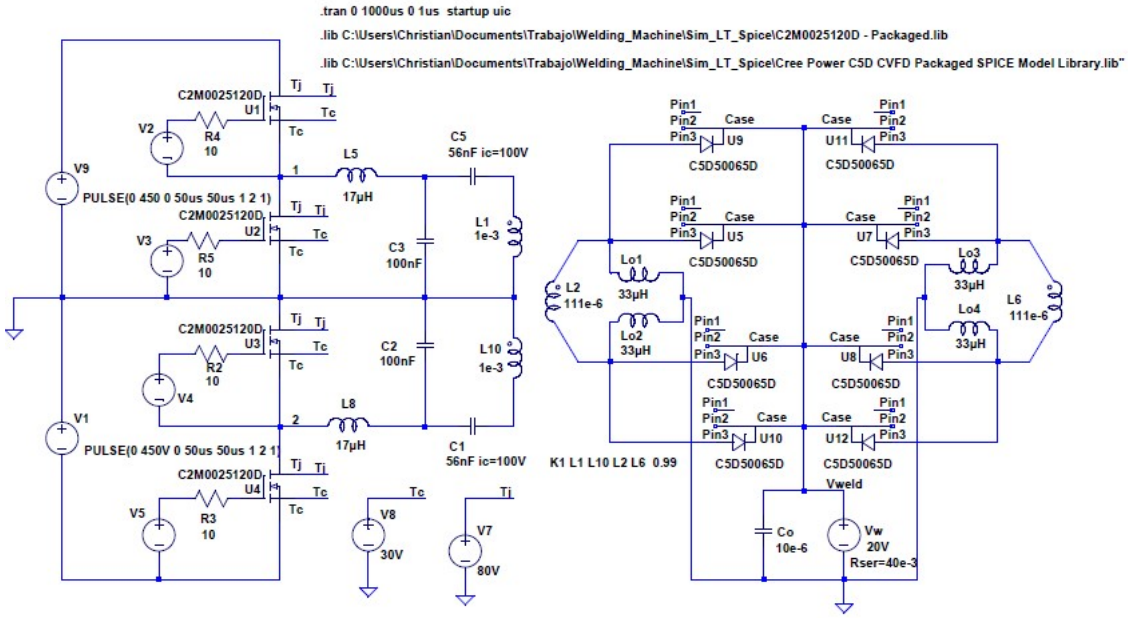

Fig.9. Implementation for simulation purposes into the LTspice IV framework of the proposed converter.

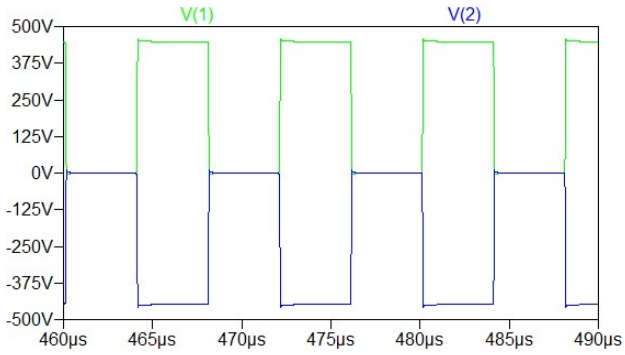

Fig. 10. Midpoint voltages v_1 and v_2 at $\Psi = 0^o$.

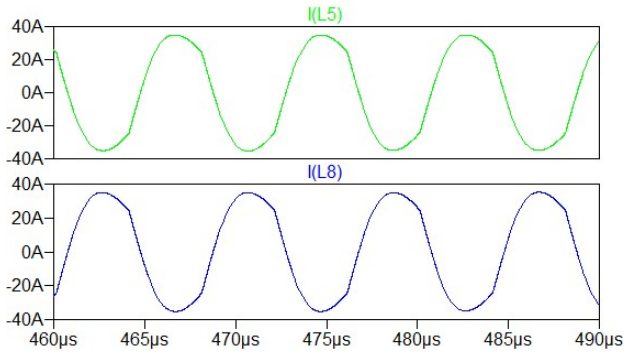

Fig. 11. Resonant currents i_1 and i_2 at $\Psi = 0^o$.

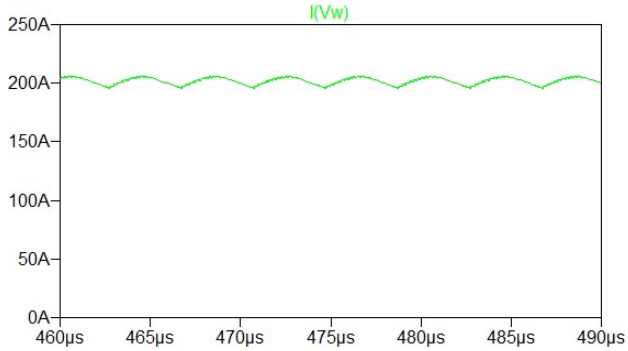

Fig. 12. Maximum welding current, I_w, achieved at $\Psi = 0º$.

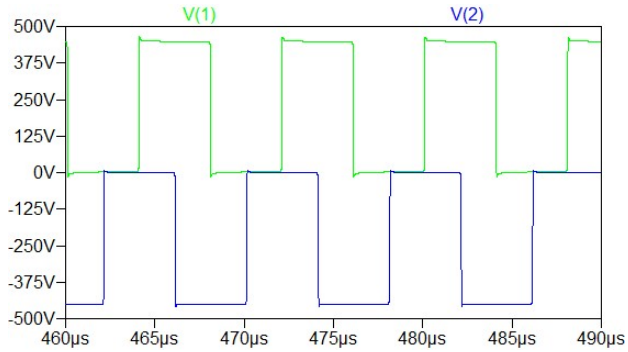

Fig. 13. Midpoint voltages v_1 and v_2 at $\Psi = 90º$.

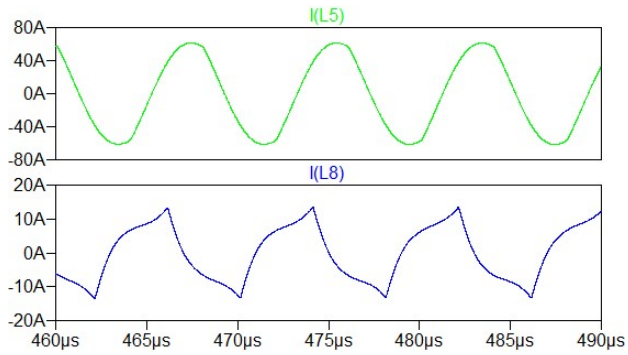

Fig. 14. Resonant currents i_1 and i_2 at $\Psi = 90º$.

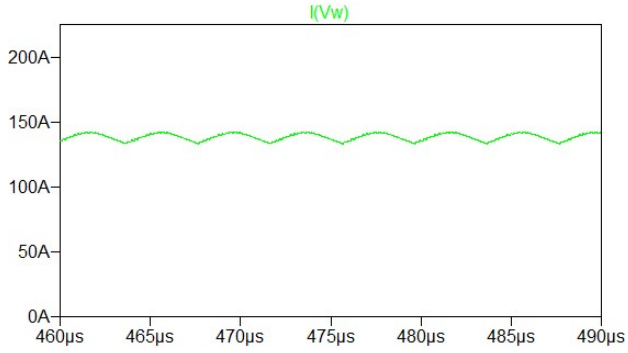

Fig. 15. Welding current at $\Psi = 90º$.

CONCLUSIONS

The analysis and design of an unfolded resonant converter for welding applications has been presented. The arc is naturally stabilized by the output impedance of the resonant tank, requiring no extra control action for this purpose. The current level control is carried out at constant frequency, by adjusting the phase displacement of the drive signals of one converter with respect to the other, which results in soft transitions preserving the arc stability. This phase-control achieves zero voltage switching (ZVS) mode at any operation point.

ACKNOWLEDGMENT

This work was funded by the Spanish Ministry of Science and the EU through the project TEC2014-52316-R: 'Estimation and Optimal Control for Energy Conversion with Digital Devices' ECOTRENDD.

REFERENCES

[1] S. Singer, "Gyrators Application in Power Processing Circuits," IEEE *Trans. on Industrial Electronics*, vol. IE-34, no. 3, pp. 313-318, Aug. 1987.

[2] Cheol-O Yeon, Jong-Woo Kim, Moo-Hyun Park, Il-Oun Lee, and Gun-Woo Moon, "Improving the Light Load Regulation Capability of LLC Series Resonant Converter using Impedance Analysis," *IEEE Trans. on Power Electronics*. Early Access.

[3] H. Pollock; J. O. Flower, "Series-parallel load-resonant converter for controlled-current arc welding power supply," *IEE Proceedings - Electric Power Applications*. vol. 143, no. 3. pp. 211-218. 1996.

[4] M. Borag, S. Tiwari, and S. Kotaiah, "LCL-T resonant converter with clamp diode- A novel constant-current power supply with inherent constant-voltage limit," *IEEE Trans. Ind. Electron.*, vol. 54, no. 21, pp. 741–746, Apr. 2007.

[5] J. Shklovski, K. Janson, and A. Kallaste, "Load-resonant converter with changing resonant tank topology for welding applications," in Proc. 38th Annu. Conf. IEEE Ind. Electron. Soc., 2012, pp. 518–524.

[6] A. Navarro, V. M. López, R. Casanueva, F. J. Azcondo, "Digital Control for an Arc Welding Machine Based on Resonant Converters and Synchronous Rectification," *IEEE Trans. Ind. Informatics*, vol. 9, no. 2, pp. 839–847, May 2013.

[7] Shinji Yamamoto; Taira Momii; Toru Iwao; Motoshige Yumoto, "Penetration depth in welding pool affected by current increment ratio in pulsed arc," *2014 IEEE 41st International Conference on Plasma Sciences* (ICOPS) held with 2014 IEEE International Conference on High-Power Particle Beams (BEAMS).

[8] Jian-Min Wang and Sen-Tung Wu, "A novel inverter for arc welding machines," *IEEE Trans. Ind. Electronics*, vol. 62, no. 3, pp.1431-1439, March 2015.

[9] Rinkle Jain; Ned Mohan; Rajapandian Ayyanar; Robert Button "A Comprehensive Analysis of Hybrid Phase-Modulated Converter With Current-Doubler Rectifier and Comparison With Its Center-Tapped Counterpart," *IEEE Trans. on Industrial Electronics*. vol. 53, no. 6, pp. 1870-1880, Dec. 2006.

[10] R. Casanueva, F. J. Azcondo, F. J. Diaz, and C. Branas, "TIG welding machines," in *IEEE Industry Applications Magazine*, vol. 17, no. 5, Sept.-Oct. 2011, pp. 53–58.

[11] Khairy Sayed, Keiki Morimoto, Soon-Kurl Kwon, Katsumi Nishida, Mutsuo Nakaoka, "DC-DC Converter with Three-Phase Power Factor Correction for Arc Welder", *8th International Conference on Power Electronics - ECCE Asia*, May 30-June 3, 2011, The Shilla Jeju, Korea, pp. 1273-1277.

[12] UNE-EN 60974-1:2013, Arc welding equipment - Part 1: Welding power sources.

[13] R. L. Steigerwald. "A Comparison of Half-Bridge Resonant Converter Topologies", *IEEE Transactions on Power Electronics*, vol. 3, no. 2, pp. 174-182, April 1988.

[14] V. M. Lopez, A. Navarro-Crespin, R. W. Schnell, C. Branas, F. J. Azcondo, R. Zane, "Current Phase Surveillance in Resonant Converters for Electric Discharge Applications to Assure Operation in Zero-Voltage-Switching Mode", *IEEE Trans. on Power Electronics,* vol. 27, 2012 , pp. 2925–2935.